Korean J. Chem. Eng., 34(4), 1229-1237 (2017)
DOI: 10.1007/s11814-016-0369-y

pISSN: 0256-1115
eISSN: 1975-7220

DeNO$_x$ performance and characteristic study for transition metals doped iron based catalysts

Lin Zhu*, Zhaoping Zhong*,†, Han Yang*, Chunhua Wang, and LixiaWang***

*Key Laboratory of Energy Thermal Conversion and Control of Ministry of Education, School of Energy and Environment, Southeast University, Nanjing, P. R. China
**College of Energy and Power Engineering, Nanjing University of Aeronautics and Astronautics, Nanjing, P. R. China
(*Received 30 June 2016 • accepted 31 December 2016*)

Abstract−Novel, environmentally-benign catalysts for selective catalytic reduction of NO$_x$ were prepared by citric method through introducing transition metal elements (Ce, Cu and Co) into iron oxide. The physical-chemical properties of different catalysts were investigated by the characterization technologies like N_2-physisorption, XRD, NH_3/NO-TPD and H_2-TPR. The results indicated that the introduction of transition metal elements increased the specific surface area and adsorption ability for reactants (NH_3 and NO$_x$). The redox capacity for the doped catalysts was improved at the same time. These characteristics all contributed to the improvement of catalytic performance. The CoFeO$_x$ catalyst exhibited the widest temperature window for SCR reaction, and the CeFeO$_x$ catalyst showed the most obvious decline of NO$_x$ conversion with the elevation of temperature above 250 °C. Water vapor inhibited the SCR activity at low temperatures and relieved the decline of NO$_x$ conversion at higher temperatures. Meanwhile, the formation of N_2O was inhibited. The pretreatment of SO_2 leaded to the sulfation of the active species for different catalysts. The decline of redox capacity and the reduction of active nitrate adsorbed species accounted for the serious loss of SCR activity at low temperatures. The abundant surface acid sites brought by the sulfation process might be the main reason for good SCR activity in the medium temperature range.

Keywords: Transition Metals, Iron, SCR, H_2O, Sulfation

INTRODUCTION

Selective catalytic reduction (SCR) with ammonia is the most efficient and economic technology for NO$_x$ removal that has been successfully applied for several decades in coal-fired power plants [1-4]. The most widely used commercial catalysts are vanadium-based catalysts like V_2O_5-WO_3/TiO_2 and V_2O_5-MoO_3/TiO_2 [1,5-7]. The undesired oxidation of SO_2 [8] is an obvious drawback for this kind of catalyst. The toxicity of vanadium pentoxide to environment and human health led the wasted catalysts to being classified as hazardous waste and to be handled differently [9,10]; thus, many researchers are focusing on the develop- ment of new vanadium-free SCR catalysts.

The environmentally-benign iron based catalysts for selective catalytic reduction of NO$_x$ have attracted much attention. Based on the abundance of published researches, the manganese based catalysts and cerium-based catalysts exhibited great SCR activity under the clean condition without H_2O and SO_2 [11-15]. The poor resistance to H_2O and SO_2 was the main barrier for the application of these novel SCR catalysts in the real environment [16,17]. The low N_2 selectivity was another drawback for the manganese-based catalysts [18]. Numerous studies have shown that the iron-based catalysts had better resistance to SO_2 in the medium temperature range. Kato et al. [19] studied the SCR performance of iron oxide-titanium oxide first and found that Fe_2O_3-TiO_2 catalysts exhibited high activity and selectivity over a temperature range of 350 °C-450 °C. The deep investigation found that the activity was enhanced with increase in the content of SO_4^{2-} in the catalyst [20]. Liu et al. [21] reported a novel iron titanate catalyst which has excellent SCR activity, N_2 selectivity and H_2O/SO_2 durability in medium temperature, and the mechanism study revealed that the SCR process mainly followed the Langmuir-Hinshelwood (L-H) mechanism in a relatively low temperature range (<200 °C) and the Eley-Rideal (E-R) mechanism at a relatively high temperature (>200 °C) [22]. In addition, Yang et al. [23] synthesized the Fe-Ti spinel catalyst that had excellent SCR activity and H_2O/SO_2 durability at 300-400 °C. Ma et al. [24] compared the SCR activities of $Fe_2(SO_4)_3$/TiO_2 and other catalysts containing iron and sulfates and found that $Fe_2(SO_4)_3$/TiO_2 catalyst exhibited the highest NO$_x$ conversion and lowest N_2O selectivity. Fe-zeolite catalysts have attracted much attention in recent years and the investigations about the activities of different iron species [25], the influence of loading [26], hydrothermally ageing [27,28] and NO_2 in the feed gas [29] have been performed by many researchers. The abundant reports have proved that the iron-based catalysts exhibited a good ability to resist the SO_2 poison to a certain extent, and the introduction of other elements might improve the reaction activity according to the published [30-32].

†To whom correspondence should be addressed.
E-mail: zzhong@seu.edu.cn
‡The paper will be reported in the 11th China-Korea Clean Energy Workshop.

Most of the published papers investigated the supported catalysts with different supporters like TiO_2, ZrO_2 and zeolites as mentioned above. To avoid the influence of the supporter, we hope to synthesize the bulk phase catalysts and investigate the mutual effect of iron and transition metal elements directly. The cerium and iron composite could be obtained by co-precipitation method with ammonia water as the precipitant [30]. However, the Co^{2+} and Cu^{2+} ions could not be precipitated by ammonia water, because that NH_4^+ could react with the corresponding cation species forming the complex ions. Using the alkali hydroxide as the precipitant will bring in the residual of alkali metal, which can lead to the poisoning of SCR catalysts. Therefore, we adopted the citric method that has been used successfully as the doping way [33,34]. In this paper, we prepared the iron-based catalysts doped by different transition metal elements (Ce, Cu and Co). The influence of different transition metal elements on the SCR activity was compared. The characterizations including N_2-physisorption, XRD, NH_3/NO-TPD and H_2-TPR were employed to analyze the physical-chemical properties of these modified catalysts. The resistance to H_2O and SO_2 was investigated and the characterization analyses for the catalysts pretreated by SO_2 were carried out to explore the deactivation reason.

EXPERIMENTAL

1. Catalyst Preparation

The $MFeO_x$ mixed oxide catalysts were prepared by the citric method. The iron nitrate nonahydrate with different transition metal nitrate (cerium nitrate hexahydrate, copper nitrate trihydrate and cobalt nitrate hexahydrate) were dissolved in deionized water first. The molar ratio of Fe and M (M=Ce, Cu and Co) was 9 : 1. The appropriate amount of nitric acid and citric acid was added into the solution, respectively. The molar ratio of metal components to citric acid to nitric acid was 1 : 1.5 : 1.5. The solutions were stirred at 80 °C for 5 h to form the gels. Then the gels were dried at 105 °C overnight and calcined in a muffle furnace at 400 °C for 3 h. The samples were pelleted, crushed and sieved to 40-60 mesh for performance evaluation and characterization. The catalysts doped by different transition metals are denoted as $MFeO_x$ (M=Ce, Cu and Co). The single metal oxides (FeO_x, CeO_x, CuO_x and CoO_x) were synthesized by the same method for comparison. The commercial Fe_2O_3 (analytical reagent) was purchased from Sinopharm Chemical Reagent Co., Ltd and labeled as Fe_2O_3 (AR). To investigate the influence of SO_2 on the properties of different catalysts, the corresponding catalysts were pretreated under the condition with 1,000 ppm SO_2 and 5 vol% O_2 at 300 °C for 4 h. The pretreated catalysts are labeled as $MFeO_x$-S (M=Ce, Cu and Co).

2. Activity Test

SCR activity tests for different catalysts were conducted in a fixed-bed stainless steel reactor (i.d 10 mm). 1.5 mL catalysts with 40-60 mesh size were used for the performance test. The simulated flue gas consisted of 500 ppm NO, 500 ppm NH_3, 3 vol% O_2 and N_2 in balance. The total flow rate was 1.5 L/min (refers to 1 atm and 25 °C), which corresponded to a gas hourly space velocity (GHSV) of 60,000 h^{-1}. When the resistance to H_2O was tested, the deionized water was injected into the preheating section by the micro syringe pump and then was vaporized and mixed with other gas components. The concentrations of NO, NO_2 and O_2 in the outlet gas were measured online by the flue gas analyzer (NOVA PLUS, MRU, Germany), while the N_2O concentration was measured by a N_2O analyzer (G200, UK). The product was analyzed when the reaction system reached a steady state for 30 min. The NO_x conversion was calculated as follows:

$$NO_x \text{ conversion} = \left(1 - \frac{[NO_x]_{out}}{[NO_x]_{in}}\right) \times 100\% \quad (1)$$

NO_x includes NO and NO_2. N_2O is classified as the undesired product.

A separate NH_3 oxidation test was performed in a quartz reactor and the GHSV was the same as SCR activity test. Different catalysts (1 mL, 40-60 mesh) were used to oxidize 300 ppm NH_3 in presence of 3 vol% O_2 catalytically. Except for monitoring the NO_x and N_2O, the outlet concentration of NH_3 was measured by ULTRAMAT6 analyzer (Siemens, Germany).

3. Catalyst Characterization

The N_2 adsorption-desorption isotherms were obtained at −196 °C using a JW-BK112 instrument (Beijing JWGB Sci. & Tech. Co., Ltd., China). Prior to N_2 adsorption, the catalyst samples were degassed at 250 °C for 5 h. The surface areas were determined by BET equation in 0.05-0.35 partial pressure range. Pore volumes and average pore diameters were determined by BJH method from the adsorption branches of the isotherms. The XRD measurements were conducted on a Rigaku D/max-RB Diffractometer (Japan, Cu K_α as radiation resource).

NH_3-TPD and NO_x-TPD were carried out using FineSorb 3010D chemisorption analyzer (FINETEC instruments, China). Prior to TPD experiments, the samples (100 mg) were pretreated at 400 °C in a flow of helium (20 mL/min) for 1 h and cooled to 80 °C. Then the samples were exposed to a flow of 5 vol% NH_3/N_2 or 5 vol% NO/N_2 (20 mL/min) for 30 min, followed by He purge for another 1 h. Finally, the temperature was raised to 500 °C in He flow at the rate of 10 °C/min. The amount of ammonia or NO_x species desorbed from the catalysts was monitored by a thermal conductivity detector (TCD).

H_2-TPR was also performed using the same instrument. Before the experiment, the catalysts (50 mg) were pretreated at 400 °C in a flow of Ar (20 mL/min) for 1 h and cooled to 50 °C. Then the temperature was raised linearly to 800 °C at the rate of 10 °C/min in a flow of 10% vol. H_2/Ar (20 mL/min). The H_2 consumption was monitored by TCD.

In situ DRIFTS spectra were measured by an FTIR spectrometer (Thermo Nicolet 6700) equipped with a diffuse reflectance optics accessory. The catalysts were pretreated at 450 °C in a flow of 5 vol% O_2/N_2 for 0.5 h and cooled to 100 °C. Thereafter, the background spectra were recorded. The 1 vol% NH_3/N_2 mixed gas was passed over the catalysts for 0.5 h and then the system was purged by N_2 for 1h. The spectra were recorded by accumulating 32 scans with a resolution of 4 cm^{-1}.

RESULTS AND DISCUSSION

1. SCR Activity

First, we tested the SCR activity of single metal oxide and the

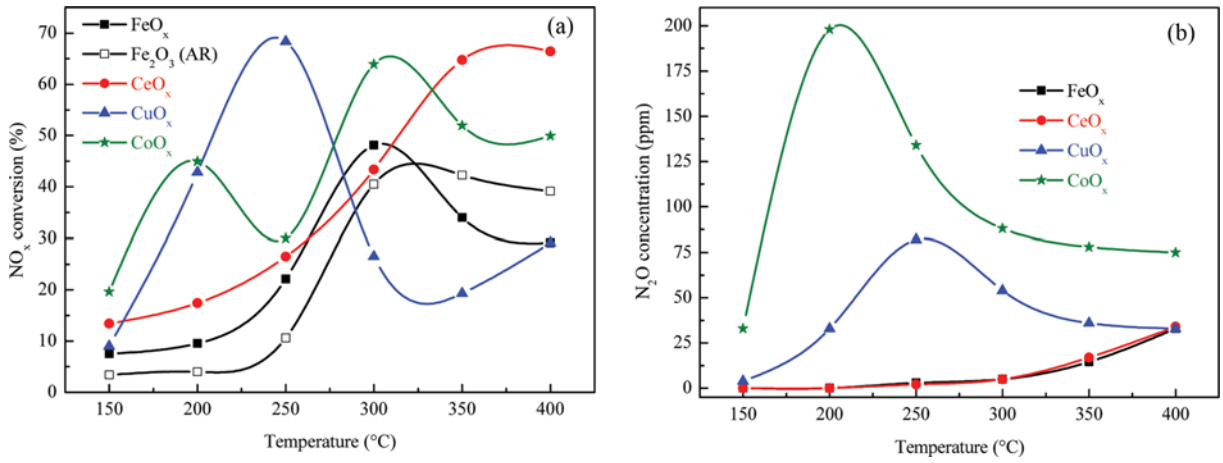

Fig. 1. NO$_x$ conversion (a) and N$_2$O concentration (b) for single metal oxides as a function of temperature. Reaction condition: [NH$_3$]=[NO]= 500 ppm, [O$_2$]=3 vol%, N$_2$ as balance, total flow rate=1.5 L/min and GHSV=60,000 h^{-1}.

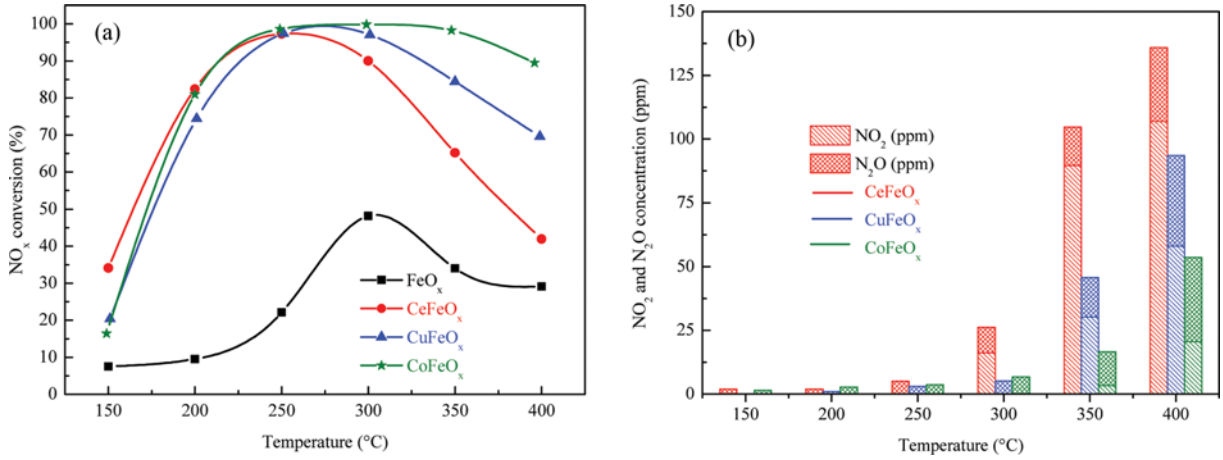

Fig. 2. NO$_x$ conversion (a), NO$_2$ and N$_2$O concentration (b) for the different catalysts as a function of temperature. Reaction condition: [NH$_3$]=[NO]=500 ppm, [O$_2$]=3 vol%, N$_2$ as balance, total flow rate=1.5 L/min and GHSV=60,000 h^{-1}.

results are shown in Fig. 1. Compared with the Fe_2O_3 (AR), the FeO_x sample exhibited the better catalytic performance at low temperature. However, the decrease of NO_x conversion was more obvious for Fe_2O_3 (AR) at higher temperature. The NO_x removal efficiency increased monotonically with the increase of reaction temperature for CeO_x. The NO_x conversion increased rapidly to a maximum at 250 °C for CuO_x sample and then decreased at higher temperature. The SCR activity for CoO_x was interesting that there were two peaks of NO_x reduction in different temperature range. Combining with the formation of N_2O, we speculated that different reaction pathways took place at different temperature. The NO might be removed through Langmuir-Hinshelwood mechanism at 200 °C. The adsorbed nitrate species reacted with the adsorbed ammonia forming NH_4NO_3 species, which could be reduced by NO to product N_2 and H_2O or decompose to N_2O and H_2O directly [22,35]. The excellent activity of cobalt species for NO oxidation in the published papers [36-38] and the trend of N_2O in the exhaust could support our speculation. When the reaction temperature rose, the stable nitrate species could not be formed. But the activation of ammonia was enhanced and NO could be reduced by active ammonia species through Eley-Rideal mechanism. To sum up, FeO_x and CeO_x samples showed better N_2 selectivity, while the catalytic activity at low temperature was worse.

The SCR activity and NO_2, N_2O concentrations in the outlet for different doped catalysts are shown in Fig. 2. The SCR activity of complex oxides catalysts was different from that of those single metal oxide samples obviously, which indicated that there were synergistic effects existing between iron and transition metal elements. The addition of transition metal elements increased the SCR activity dramatically compared with FeO_x and there was a deep increase between 150 °C and 200 °C for these modified catalysts. The temperature corresponding to the highest NO_x conversion shifted from 300 °C to 250 °C and the deNO_x efficiencies all exceeded 95% at 250 °C for the series of $MFeO_x$ catalysts. When the temperature reached 300 °C, the NO_x conversion of $CeFeO_x$ and $CuFeO_x$ started to decrease. The degree of decline was enhanced with the increase of temperature and it was more serious for $CeFeO_x$ catalyst compared with the $CuFeO_x$ sample. The turning point for $CoFeO_x$ cat-

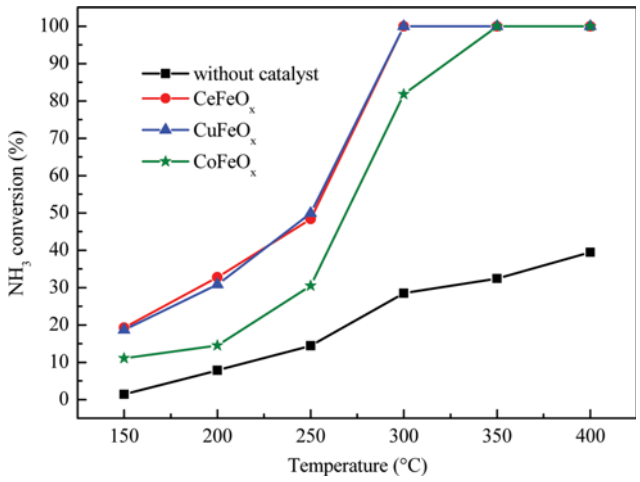

Fig. 3. NH_3 conversion for the different catalysts as a function of temperature. Reaction condition: $[NH_3]$=300 ppm, $[O_2]$=3 vol%, N_2 as balance, total flow rate=1.0 L/min and GHSV= 60,000 h^{-1}.

alyst was at 350 °C and its rate for decrease was smallest. The decrease of NO_x conversion at high temperature might be due to the over-oxidation of ammonia [21,32].

To confirm our speculation, a separate NH_3 oxidation test was performed for these modified catalysts and the results are shown in Fig. 3. The blank test showed that ammonia was not stable in the presence of O_2 at higher temperature. The existence of catalysts could improve the NH_3 oxidation conversion. The NH_3 oxidation activities for $CeFeO_x$ and $CuFeO_x$ catalysts were similar that the NH_3 conversion increased rapidly when the temperature was over 250 °C and reached 100% at 300 °C. The NH_3 conversion for $CoFeO_x$ was lower and reached 100% at 350 °C. The temperature for complete NH_3 oxidation was in accord with that for decline of $deNO_x$ efficiency under SCR condition, which could support our speculation. Interestingly, there was almost no N_2O detected in the exhaust. Different proportions of NO and NO_2 were monitored only at 400 °C.

It can be seen in Fig. 2(b) that only small amount of N_2O was detected at the temperature below 250 °C under SCR condition. The NO_2 in the outlet appeared for $CeFeO_x$ catalysts at 300 °C, which corresponded to the temperature that NO_x conversion started to decrease. The concentration of NO_2 increased gradually with the temperature rising. Due to the over-oxidation ammonia, NO could not be reduced without enough reductant (NH_3) and then was oxidized to NO_2. This phenomenon indicated the good NO oxidation performance for the doped catalysts. The N_2O formation in the temperature range investigated was similar for the different catalysts, and the concentration of N_2O reached the maximum (approximate 30 ppm) at 400 °C. Combined with the results of NH_3 oxidation, we think that the N_2O came from the unselective catalytic reduction of NO instead of direct NH_3 oxidation.

2. Catalyst Characterization

2-1. N_2 Physisorption and XRD

The structural parameters of the different catalysts are listed in Table 1. It can be seen that the addition of transition metals increased

Table 1. Structural parameters of different catalysts

Sample	BET surface area (m^2/g)	Total pore volume (cm^3/g)	Average pore diameter (nm)
FeO_x	19.32	0.287	51.34
$CeFeO_x$	130.81	0.244	6.76
$CuFeO_x$	37.93	0.172	19.23
$CoFeO_x$	40.70	0.241	18.86

the specific surface areas. The physical structures showed diverse changes for the novel catalytic materials with different doped elements. The specific surface area of the FeO_x sample was smallest and its pore was mainly macropore. The average pore diameter decreased for the doped catalysts and more mesoporous structure appeared. The $CeFeO_x$ catalyst had the smallest average pore diameter and biggest BET surface area, while the $CuFeO_x$ and $CoFeO_x$ catalysts had similar physical structural parameters. According to the atomic radii proposed by Slater [39], it is easy to find that the iron, copper and cobalt have a similar atomic radius (Fe: 0.14 nm; Cu: 0.135 nm and Co: 0.135 nm), while the atomic radius of cerium is 0.185nm. The obvious difference between the atomic radius of Ce and Fe might lead to more crystal distortion. The smallest average pore diameter of $CeFeO_x$ was a valid proof for this deduction, and these small pore structures enlarged the specific surface area for the catalyst. The increase of specific surface area and adjustment of pore structure both could contribute to the improvement of catalytic performance.

Fig. 4 shows the XRD profiles of different catalysts. For FeO_x catalyst, the crystal Fe_2O_3 was detected obviously, corresponding to the standard card (PDF 89-0597) in JCPDS. After the introduction of transition metals, the position and intensity of diffraction peaks for the doped catalysts changed significantly. Apart from the typical diffraction peak at 33.12° for crystal Fe_2O_3, most diffraction peaks were attributed to the formation of maghemite $Fe_{21.333}O_{32}$ (PDF 83-0112). The transformation of the main crystal form indicated that the addition of transition metals affected the physical-

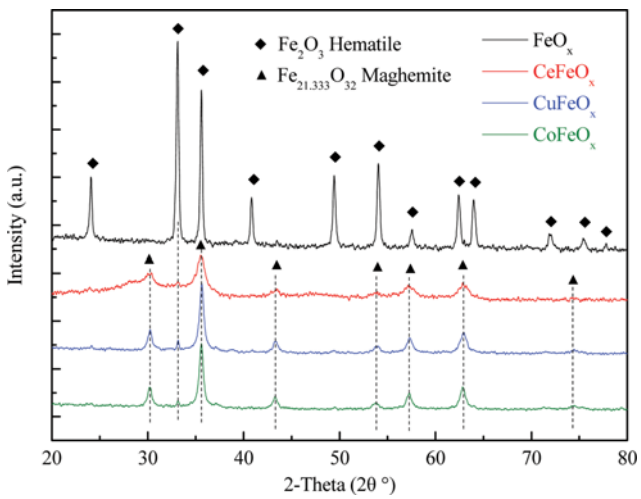

Fig. 4. XRD profiles for the different catalysts.

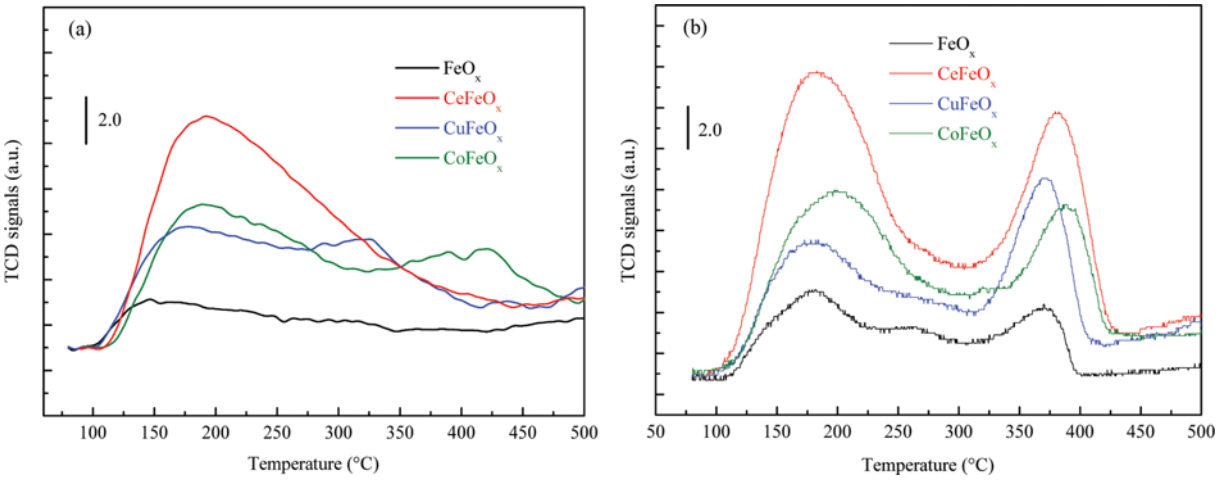

Fig. 5. NH_3-TPD and NO-TPD profiles for the different catalysts.

chemical characteristic of iron-based materials and more crystal defect existed on the doped catalysts. Comparing these materials, the weakest diffraction peaks was for $CeFeO_x$ catalyst, which might be because the bigger atomic radius for cerium element reduced the degree of crystallization. There were no crystal diffraction peaks for the added transition metal oxides, which suggested that they were dispersed well on the surface of catalysts.

2-2. NH_3-TPD and NO-TPD

According to the numerous investigations on the iron-based SCR catalysts, the adsorbed ammonia species and nitrate species showed reaction activity at different temperatures [22,23,40]. The adsorption of reactants on the surface of catalysts is a very important factor for the SCR performance of novel catalysts. The NH_3-TPD and NO-TPD profiles for the different catalysts are shown in Fig. 5. It is easy to find that the addition of transition metals clearly increased the adsorbing capacity of the reactants. The bigger specific surface area was a reason for the increase of adsorption ability. However, the amount of reactants was out of proportion with the BET surfaces, which indicated that the chemical properties changed by the doping of transition metal elements. The $CeFeO_x$ catalyst exhibited the best adsorption capacity for NH_3 and NO_x. The excellent oxygen storage ability of cerium contributed to the adsorption and activation of the reactants, which could explain the great oxidation performance for ammonia and NO during the activity test process. The broad peak between 350 °C and 450 °C in NH_3-TPD profile showed that more strong Lewis acid sites existed on the surface of $CoFeO_x$ catalyst, and the desorption temperature for different nitrate species was higher than that of the other two modified catalysts, which indicated that the thermal stability for adsorbed ammonia and nitrate species was better for $CoFeO_x$ catalyst. This characteristic of $CoFeO_x$ catalyst prevented the over-oxidation of ammonia at high temperature, leading to the better SCR activity. Combining with the result of activity test, we speculated that there was a relation between the thermal stability of adsorbed ammonia and the ammonia oxidation ability of the novel catalysts.

2-3. H_2-TPR

The redox capacity is another critical property for the selective

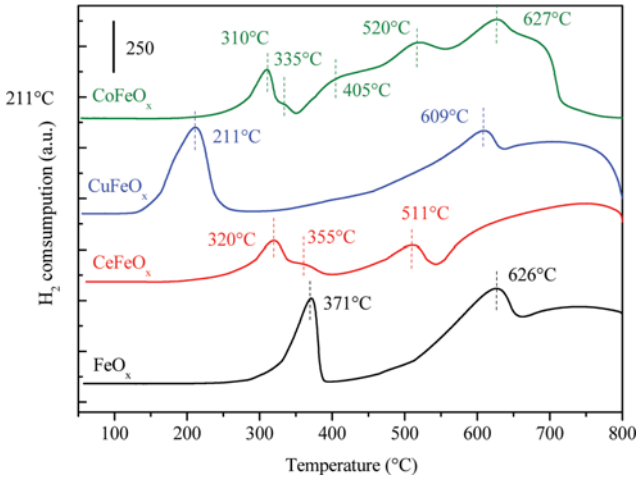

Fig. 6. H_2-TPR profiles for the different catalysts.

catalytic reduction of NO with ammonia. Temperature-programmed reduction (TPR) technology was used to investigate the reducibility of the different catalysts, and the corresponding curves are shown in Fig. 6. The SCR reaction was operated below 500 °C, so the oxidation-reduction reaction that happened on the different catalysts during the SCR reaction may be only related to the reduction of low temperature. Therefore, we focused on the analysis of reduction peaks at low temperature. The first reduction temperature at 371 °C for FeO_x was attributed to the sequential reduction of highly dispersive Fe_2O_3 to Fe_3O_4 [21,24]. The broad reduction peaks above 500 °C were attributed to the further reduction of Fe_3O_4, FeO, crystallized and bulk iron oxides [21,31]. Three different reduction peaks were found for $CeFeO_x$ catalyst. As reported, the reduction peak at 511 °C was due to the reduction of Ce^{4+} to Ce^{3+} [41]. The reduction peak at 355 °C corresponded to the shift of peak at 371 °C for FeO_x. The new peak at 320 °C was caused by the strong interaction between FeO_x and CeO_x and could be assigned to the superimposed reduction of active cerium ions and iron ions [42]. The sole reduction peak at 211 °C for $CuFeO_x$ catalyst at low temperature was due to the overlap for the reduction of highly dispersed

copper oxides and iron oxides [32,43,44], which indicated the close interaction between Cu and Fe species existed. There were various reduction peaks for $CoFeO_x$ catalyst, suggesting that different oxide forms existed. The first and second reduction peaks at 310 °C and 335 °C were superimposed by the reduction of highly dispersed Co_3O_4 and Fe_2O_3, which were both lower than the single component samples [45]. The reduction peaks at 405 °C and 520 °C were attributed to the overlapped reduction of CoO, FeO and crystallized iron species [31,37]. Different from the other catalysts, $CoFeO_x$ sample was almost totally reduced below 800 °C. We speculated that the addition of cobalt as the adjacent subgroup element of iron greatly impacted the physical-chemical property of iron oxides.

Compared with the FeO_x catalyst, the introduction of Ce, Cu and Co all decreased the reduction temperature of active iron species, and the interaction between the doped elements and iron increased the redox capacity for the modified catalysts, contributing to the improvement of SCR activity.

3. Effect of H_2O and SO_2

The effects of water vapor on the NO_x conversion and N_2O formation of the different catalysts are shown in Fig. 7. Clearly, the existence of H_2O inhibited the SCR activity at low temperature. The NO_x conversion of $CuFeO_x$ and $CoFeO_x$ decreased from 74.4%, 81.0% to 26.0% and 23.0% at 200 °C, respectively, while the denitration efficiency of $CeFeO_x$ could still keep at 49.0% at 200 °C. The inhibition of H_2O was reversible for all the doped catalysts, and the original catalytic performance could be recovered as the addition of water vapor was stopped [46,47]. As the reaction temperature rose, the degree of inhibition was reduced. The NO_x conversion at 250 °C in presence of H_2O was close to that at 200 °C in absence of H_2O. The temperature for turning point of NO_x conversion shifted from 300 °C to 350 °C and the decrease of SCR activity at high temperature for $CuFeO_x$ and $CeFeO_x$ was weakened dramatically. The suppression of adsorption and activation of reactants (ammonia and nitric oxide) was the main reason for the loss of activity at low temperature. The inhibition for over-oxidation of ammonia contributed to the activity improvement at high temperatures.

The NO_2 was detected at 300 °C for $CeFeO_x$ catalyst under the

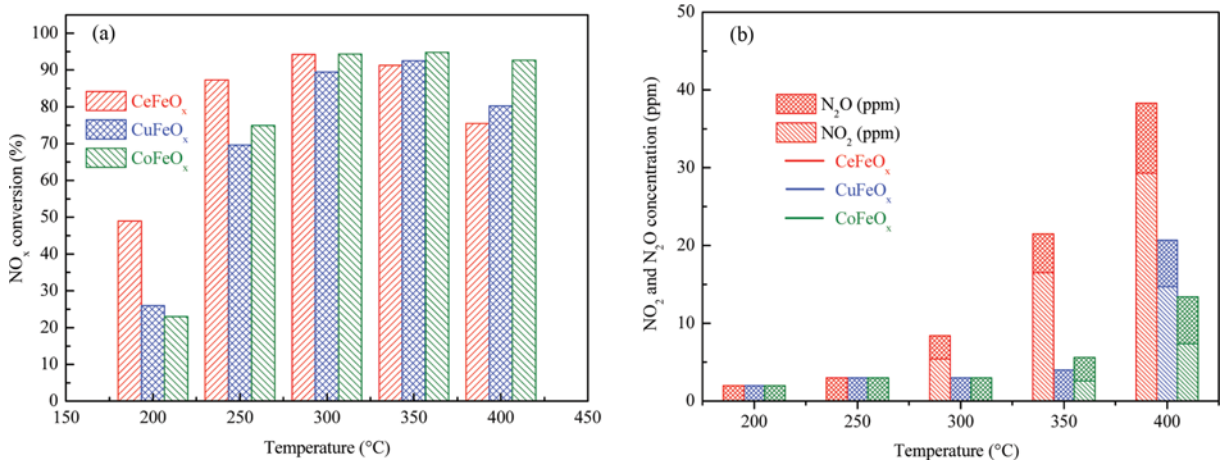

Fig. 7. NO_x conversion (a), NO_2 and N_2O concentration (b) for the different catalysts as a function of temperature. Reaction condition: $[NH_3]=[NO]=500$ ppm, $[O_2]=3$ vol%, $[H_2O]=5$ vol%, N_2 as balance, total flow rate=1.5 L/min and GHSV=60,000 h^{-1}.

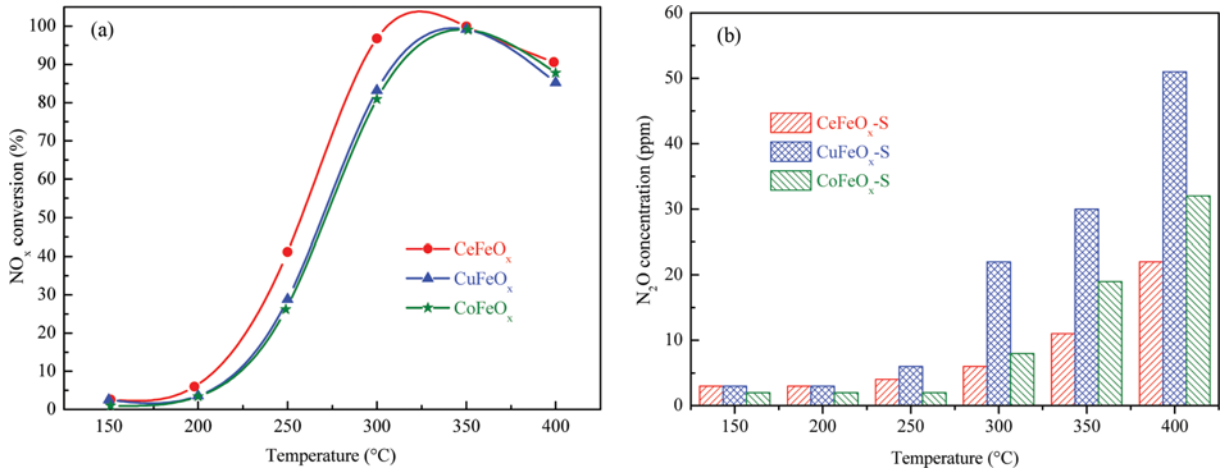

Fig. 8. NO_x conversion (a) and N_2O concentration (b) for the different catalysts pretreated by SO_2 as a function of temperature. Reaction condition: $[NH_3]=[NO]=500$ ppm, $[O_2]=3$ vol%, N_2 as balance, total flow rate=1.5 L/min and GHSV=60,000 h^{-1}.

wet condition, which was in agreement with the phenomenon in absence of H_2O. However, the concentration of NO_2 decreased significantly (107 ppm at 400 °C in absence of H_2O vs. 29 ppm at 400 °C in presence of H_2O). The influence for $CuFeO_x$ catalyst was similar to that for $CeFeO_x$ and the NO_2 was obvious only at 400 °C. The N_2O concentration for different modified catalysts kept in the same level and the existence of water vapor inhibited the formation of N_2O. Below 10 ppm N_2O was detected for these catalysts at 400 °C.

The SO_2-pretreated catalysts exhibited the different reaction activity in the temperature range investigated and the influence brought by the pretreatment of SO_2 was irreversible. The reaction activity at low temperatures was lost almost as shown in Fig. 8. The $CuFeO_x$ and $CoFeO_x$ catalysts showed the close NO_x conversion at different temperature and NO_x removal efficiency above 80% was only obtained between 300 °C and 400 °C. The NO_x conversion for $CeFeO_x$ catalyst was slightly higher than the others at the same temperature. It is interesting that there was no NO_2 in the outlet even at 400 °C, which indicated that the SO_2-pretreated catalysts lost the ability for NO oxidation. The trend for N_2O formation of different catalysts was in accordance with the fresh catalysts that the N_2O concentration increased with the elevation of reaction temperature. However, the order for N_2O concentration changed. The SO_2-pretreated $CuFeO_x$ catalyst produced the most N_2O byproduct above 300 °C, which was more than the corresponding fresh catalyst.

4. Characterization for Catalysts Pretreated by SO_2

To confirm the reason for the impacts brought by the pretreatment of SO_2 on the different modified catalysts, temperature-programmed desorption (NH_3/NO-TPD) and temperature-programmed reduction (H_2-TPR) technologies were carried out for the SO_2-pretreated catalysts. The change of adsorption ability and reducibility could be obtained compared with the fresh catalysts in Section 2.

4-1. NH_3-TPD and NO-TPD

The NH_3/NO-TPD profiles for the SO_2-pretreated catalysts are shown in Fig. 9. Compared with Fig. 5, the amount for NH_3 adsorbed species increased dramatically for the SO_2-pretreated catalysts. There was a big broad peak between 100 °C and 500 °C for $CeFeO_x$-S catalysts. The NH_3-TPD profile of SO_2-pretreated $CoFeO_x$ catalyst was similar to that of the fresh sample, and the temperature for the second desorption peak shifted towards higher temperature. The SO_2-pretreated $CuFeO_x$ catalyst exhibited some new special desorption peaks, which might be attributed to the desorption of ammonia species adsorbed on copper sulfate. Combined with the change of SCR activity, the total amount of surface acid sites was not the determinant for NO_x removal. It can be seen that there was only one desorption peak for NO_x adsorbed species of these SO_2-pretreated catalysts. The pretreatment of sulfur dioxide in presence of oxygen inhibited the absorption of nitrate species, especially bidentate nitrate and bridging nitrate with better thermal stability. The sulfated catalysts did not show enough NO_x conversion in the temperature range for desorption of nitrate adsorbed species, which suggested that the nitrate adsorbed species did not have reaction activity for NO_x removal. The same conclusion was obtained by Liu et al. [48] on the $FeTiO_x$ catalyst, that the active nitrate species could not form effectively owing to the strong acidity of sulfate species on iron sites.

Based on the change of adsorption capacity for NH_3 and NO_x species, it could be concluded that sulfur dioxide bonded with the surface of different catalysts strongly during the pretreatment process and some reaction might happen between SO_2 and the surface active species in presence of excess O_2.

4-2. H_2-TPR

The SO_2-pretreated catalysts exhibited the different H_2-TPR profiles compared with the fresh catalysts as shown in Fig. 10. It was obvious that all the initial reduction temperature shifted towards the higher temperature and the amount of H_2 consumption for the first reduction peak increased dramatically. The first reduction peak for $CeFeO_x$-S and $CoFeO_x$-S catalysts appeared at 492 °C and 410 °C respectively and they were overlapped by the reduction peaks for different species. The surface sulfate species were reduced by hydrogen firstly and then the corresponding metal oxides were reduced immediately. As the temperature continued increasing, the profile of H_2 consumption became similar with that of fresh catalysts. The $CuFeO_x$-S catalyst showed two distinctive reduction

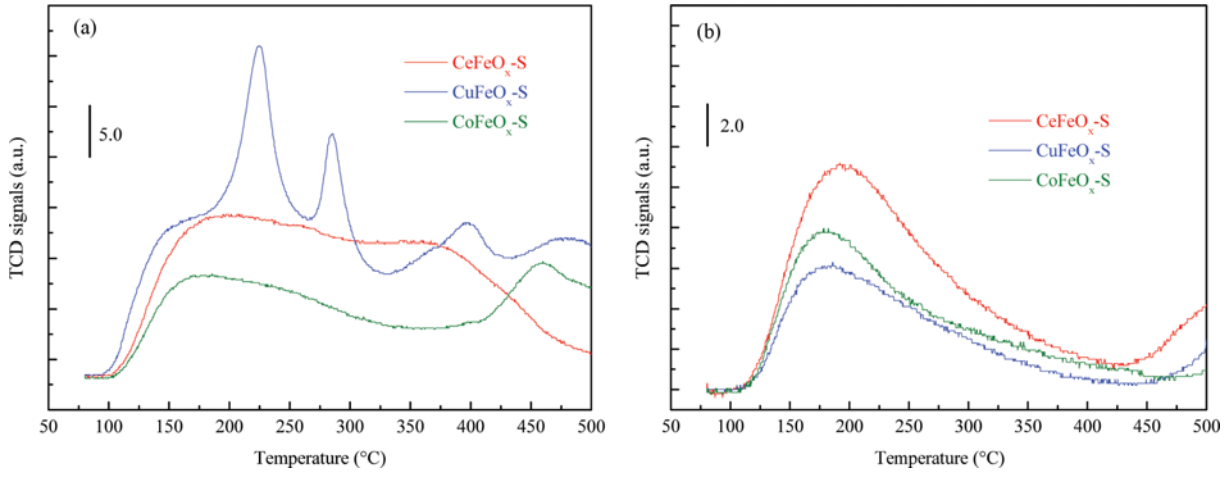

Fig. 9. NH_3-TPD and NO-TPD profiles for the SO_2-pretreated catalysts.

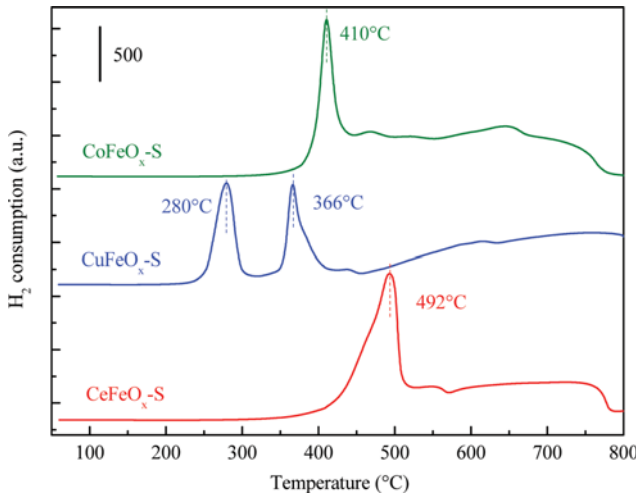

Fig. 10. H_2-TPR profiles for the SO_2-pretreated catalysts.

peaks and the pretreatment of SO_2 might separate the reduction process for copper oxides and iron oxides. The first reduction peak at 280 °C was attributed to the superimposed reduction of the sulfate species on CuO_x and highly dispersed copper oxides, while the second reduction peak at 366 °C was assigned to the reduction of the sulfate species on iron oxides and corresponding iron oxides. We deduced that the sulfation of active species reduced the redox capacity of different catalysts and the reduction for surface sulfate accounted for the most of H_2 consumption.

4-3. IR Spectra

Interestingly, the pretreatment of SO_2 increased the acid sites for the modified catalysts, which did not improve the catalytic performance. Due to the defect of TCD detector for identifying the type of acid sites, the change for different kind of acid sites could not be obtained from NH_3-TPD profiles. The *in situ* DRIFT spectra recorded for $CeFeO_x$ and $CeFeO_x$-S catalysts at 100 °C are shown in Fig. 11. After NH_3 adsorption and N_2 purge, the $CeFeO_x$ catalyst

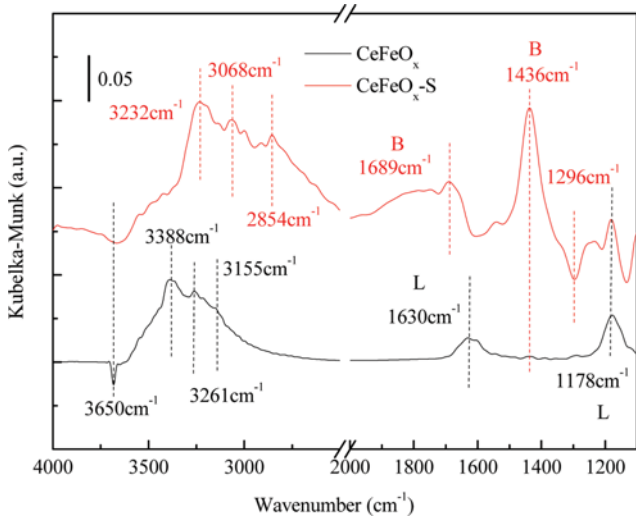

Fig. 11. DRIFT spectra for the fresh and SO_2-pretreated $CeFeO_x$ catalysts.

was mainly covered by coordinated NH_3 bound to Lewis acid sites (1,178 cm^{-1} for $\delta_s NH_3$ the and 1,630 cm^{-1} for $\delta_{as} NH_3$) [22,40]. There was almost no ionic NH_4^+ bound to Brønsted acid sites on the surface of $CeFeO_x$ catalyst. The bands at 3,100-3,400 cm^{-1} (3,155, 3,261 and 3,380 cm^{-1}) were attributed to N-H stretching vibration modes for the coordinated NH_3 and the negative band at 3,650 cm^{-1} was due to the consumption of the surface O-H stretching [22,23]. The spectrum for $CeFeO_x$-S catalyst was different with that for the fresh sample. The intensity of IR bands for the coordinated NH_3 on the Lewis acid sites was weakened and strong IR bands for ionic NH_4^+ bound to Brønsted acid sites (1,436 cm^{-1} for $\delta_{as} NH_4^+$, 1,689 cm^{-1} for $\delta_s NH_4^+$ and 3,068 cm^{-1}, 2,854 cm^{-1} for N-H stretching vibration) appeared obviously [40,49]. The results indicated the increase of amount of acid sites, which was in agreement with NH_3-TPD results. The negative IR band at 1,296 cm^{-1} was near the 1,309 cm^{-1} for the sulfate and bisulfate species reported by Xu et al. [17]. The bands at 1,689 cm^{-1} and 1,436 cm^{-1} for NH_4^+ originated from the ammonia bound to the sulfate and bisulfate species and the coverage of ionic NH_4^+ led to the emergence of the negative band at 1,296 cm^{-1}.

The IR spectra confirmed the occurrence of sulfation of active species. As reported, it is generally accepted that NO could be reduced by NH_3 through the Langmuir-Hinshelwood (L-H) mechanism and Eley-Rideal (E-R) mechanism [22,49]. The adsorption and activation of ammonia is the key step for the E-R mechanism, while the formation of active nitrate species is recognized as the important step for the L-H mechanism. The sulfation of active species lost the excellent redox capacity for these catalysts, judging from the TPR-profiles. The activation of coordinated NH_3 was limited for the pretreated catalysts. And at the same time, the formation of active nitrate species was inhibited. The two pathways for NO_x removal were both cut off for these catalysts pretreated by SO_2. So, in accordance with the experimental result, the SCR activity at low temperature decreased dramatically. The abundant surface acid sites and high reaction temperature kept the good NO_x conversion in the medium temperature range. We speculated NO_x was reduced by NH_3 through the route of E-R mechanism for the sulfated catalysts.

CONCLUSION

Environmentally-benign iron based catalysts for selective catalytic reduction of NO_x have attracted considerable attention. We have investigated the deNO_x performance and physical-chemical properties of the novel $MFeO_x$ mixed oxides catalysts (M=Ce, Cu, Co) prepared by citric method. The characterization results indicated that the introduction of transition metal elements increased the specific surface area and adsorption ability for reactants (NH_3 and NO_x). The redox capacity for the doped catalysts was improved at the same time. These characteristics all contributed to the improvement of catalytic performance. The $CoFeO_x$ catalyst exhibited the widest window temperature for SCR reaction. The $CeFeO_x$ catalyst showed the most obvious decrease of NO_x conversion with the elevation of temperature, and excellent NO oxidation efficiency was observed at higher temperatures. The declining degree of NO_x conversion at higher temperatures was in line with the sequence of

thermal stability for ammonia adsorbed species on the different catalysts. Water vapor inhibited the SCR activity at low temperatures and relieved the decline of NO_x conversion at higher temperatures. Meanwhile, the formation of N_2O was inhibited. The pretreatment of SO_2 leaded to the sulfation of the active species for different catalysts. The decline of redox capacity and the reduction of active nitrate adsorbed species accounted for the serious loss of SCR activity at low temperatures. The abundant surface acid sites brought by the sulfation process might be the main reason for good SCR activity in the medium temperature range.

ACKNOWLEDGEMENTS

This research was financially supported by the Policy-induced Project of Jiangsu Province for the Industry-University-Research Cooperation (BY2015070-21) and the Natural Science Fund Program of Jiangsu Province (BK20150749).

REFERENCES

1. G. Busca, L. Lietti, G. Ramis and F. Berti, *Appl. Catal. B: Environ.*, **18**, 1 (1998).
2. V. I. Pârvulescu, P. Grange and B. Delmon, *Catal. Today*, **46**, 233 (1998).
3. P. Forzatti, *Appl. Catal. A: Gen.*, **222**, 221 (2001).
4. S. Roy, M. S. Hegde and G. Madras, *Appl. Energy*, **86**, 2283 (2009).
5. L. Lietti, J. L. Alemany, P. Forzatti, G. Busca, G. Ramis, E. Giamello and F. Bregani, *Catal. Today*, **29**, 143 (1996).
6. L. Lietti, I. Nova, G. Ramis, L. Dall'Acqua, G. Busca, E. Giamello, P. Forzatti and F. Bregani, *J. Catal.*, **187**, 419 (1999).
7. L. Lietti, I. Nova and P. Forzatti, *Topic Catalysis*, **11**, 111 (2000).
8. J. P. Dunn, P. R. Koppula, H. G. Stenger and I. E. Wachs, *Appl. Catal. B: Environ.*, **19**, 103 (1998).
9. M. Marafi and A. Stanislaus, *J. Hazard. Mater.*, **101**, 123 (2003).
10. Z. P. Zhao, M. Guo and M. Zhang, *J. Hazard. Mater.*, **286**, 402 (2015).
11. B. Q. Jiang, Y. Liu and Z. B. Wu, *J. Hazard. Mater.*, **162**, 1249 (2009).
12. M. Kang, J. H. Park, J. S. Choi, E. D. Park and J. E. Yie, *Korean J. Chem. Eng.*, **24**, 191 (2007).
13. B. Thirupathi and P. G. Smirniotis, *Appl. Catal. B-Environ.*, **110**, 195 (2011).
14. W. P. Shan and H. Song, *Catal. Sci. Technol.*, **5**, 4280 (2015).
15. C. Lei, S. Zhichun, W. Xiaodong, W. Duan, R. Rui and Y. Jun, *J Rare Earth.*, **32**, 907 (2014).
16. B. Q. Jiang, Z. B. Wu, Y. Liu, S. C. Lee and W. K. Ho, *J. Phys. Chem. C*, **114**, 4961 (2010).
17. W. Q. Xu, H. He and Y. B. Yu, *J. Phys. Chem. C*, **113**, 4426 (2009).
18. Z. M. Liu, Y. Yi, S. X. Zhang, T. L. Zhu, J. Z. Zhu and J. G. Wang, *Catal. Today*, **216**, 76 (2013).
19. A. Kato, S. Matsuda, F. Nakajima, M. Imanari and Y. Watanabe, *J. Phys. Chem.*, **85**, 1710 (1981).
20. A. Kato, S. Matsuda and T. Kamo, *Ind. Eng. Chem. Prod. Res. Develop.*, **22**, 406 (1983).
21. F. D. Liu, H. He, C. B. Zhang, Z. C. Feng, L. R. Zheng, Y. N. Xie and T. D. Hu, *Appl. Catal. B: Environ.*, **96**, 408 (2010).
22. F. D. Liu, H. He, C. B. Zhang, W. P. Shan and X. Y. Shi, *Catal. Today*, **175**, 18 (2011).
23. S. Yang, J. Li, C. Wang, J. Chen, L. Ma, H. Chang, L. Chen, Y. peng and N. Yan, *Appl. Catal. B: Environ.*, **117-118**, 73 (2012).
24. L. Ma, J. H. Li, R. Ke and L. X. Fu, *J. Phys. Chem. C*, **115**, 7603 (2011).
25. S. Brandenberger, O. Kröcher, A. Tissler and R. Althoff, *Appl. Catal. B: Environ.*, **95**, 348 (2010).
26. I. Ellmers, R. Pérez Vélez, U. Bentrup, W. Schwieger, A. Brückner and W. Grünert, *Catal. Today*, **258**, 337 (2011).
27. X. Y. Shi, F. D. Liu, L. J. Xie, W. P. Shan and H. He, *Environ. Sci. Technol.*, **47**, 3293 (2013).
28. H.-T. Lee and H.-K. Rhee, *Korean J. Chem. Eng.*, **19**, 574 (2002).
29. M. Devadas, O. Kröcher, M. Elsener, A. Wokaun, N. Söger, M. Pfeifer, Y. Demel and L. Mussmann, *Appl. Catal. B: Environ.*, **67**, 187 (2006).
30. Z. B. Xiong, C. M. Lu, D. X. Guo, X. L. Zhang and K. H. Han, *J. Chem. Technol. Biotechnol.*, **88**, 1258 (2013).
31. S. Y. Jiang and R. X. Zhou, *Fuel. Process. Technol.*, **133**, 220 (2015).
32. A. Sultana, M. Sasaki, K. Suzuki and H. Hamada, *Catal. Commun.*, **41**, 21 (2013).
33. C. C. Zhou, Y. P. Zhang, X. L. Wang, H. T. Xu, K. Q. Sun and K. Shen, *J. Colloid Interface Sci.*, **319**, 392 (2013).
34. L. Chen, Z. C. Si, X. D. Wu, D. Weng and Z. W. Wu, *J. Environ. Sci.*, **240**, 31 (2015).
35. L. Zhu, Z. P. Zhong, H. Yang and C. H. Wang, *J. Colloid Interface Sci.*, **478**, 11 (2016).
36. D. H. Shang, Q. Zhong and W. Cai, *Appl. Surf. Sci.*, **325**, 211 (2015).
37. D. H. Shang, Q. Zhong and W. Cai, *J. Mol. Catal. A-Chem.*, **399**, 18 (2015).
38. M. M. Yung, E. M. Holmgreen and U. S. Ozkan, *J. Catal.*, **247**, 356 (2007).
39. J. C. Slater, *J. Chem. Phys.*, **41**, 3199 (1964).
40. Y. Shu, H. Sun, X. Quan and S. Chen, *J. Phys. Chem. C*, **116**, 25319 (2012).
41. S. P. Ding, F. D. Liu, X. Y. Shi, K. Liu, Z. H. Lian, L. J. Xie and H. He, *ACS Appl. Mater. Inter.*, **7**, 9497 (2015).
42. X. Gao, X. S. Du, L. W. Cui, Y. C. Fu, Z. Y. Luo and K. F. Cen, *Catal. Commun.*, **12**, 255 (2010).
43. P. M. Sreekanth and P. G. Smirniotis, *Catal Lett.*, **122**, 37 (2008).
44. H. Y. Zhu, Y. Wu, X. Zhao, H. Q. Wan, L. J. Yang, J. M. Hong, Q. Yu, L. Dong, Y. Chen, C. Jian, J. Wei and P. H. Xu, *J. Mol. Catal. A: Chem.*, **243**, 24 (2006).
45. J. Liu, Z. Zhao, J. Q. Wang, C. M. Xu, A. J. Duan, G. Y. Jiang and Q. Yang, *Appl. Catal. B: Environ.*, **84**, 185 (2008).
46. S. K. Wu, H. L. Li, L. Q. Li, C. Y. Wu, J. Y. Zhang and K. Shih, *Fuel*, **159**, 876 (2015).
47. Z. H. Lian, F. D. Liu, H. He, X. Y. Shi, J. Y. Mo and Z. B. Wu, *Chem. Eng. J.*, **250**, 390 (2014).
48. F. D. Liu, K. Asakura, H. He, W. P. Shan, X. Y. Shi and C. B. Zhang, *Appl. Catal. B: Environ.*, **103**, 369 (2011).
49. L. Chen, J. H. Li and M. Ge, *Environ. Sci. Technol.*, **44**, 9590 (2010).